# Dielectrophoresis of Proteins in Solution

| | |
|---|---|
| Journal: | *The Journal of Physical Chemistry* |
| Manuscript ID | jp-2020-09007m.R1 |
| Manuscript Type: | Article |
| Date Submitted by the Author: | n/a |
| Complete List of Authors: | Heyden, Matthias; Arizona State University, School of Molecular Sciences<br>Matyushov, Dmitry; Arizona State University, School of Molecular Sciences |
| | |

# Dielectrophoresis of Proteins in Solution

Matthias Heyden*,† and Dmitry V. Matyushov*,‡

†*School of Molecular Sciences, Arizona State University, PO Box 871604, Tempe, AZ 85287-1604*

‡*Department of Physics and School of Molecular Sciences, Arizona State University, PO Box 871504, Tempe, AZ 85287-1504*

E-mail: mheyden1@asu.edu; dmitrym@asu.edu

**Abstract**

A nonionic particle placed in the gradient of an electric field experiences the dielectrophoretic force which scales linearly with the gradient of the electric field squared. The proportionality constant is the dielectrophoretic susceptibility, a linear transport coefficient. For proteins in solution, it is mostly affected by two parameters: the squared dipole moment and the cavity susceptibility accounting for cross-correlations of the protein dipole with the hydration shell (protein-water Kirkwood factor). Both these parameters enter the dielectric increment of the solution which fully specifies the dielectrophoretic susceptibility. The link between these two measurable properties is proven here to hold using molecular dynamics simulations of solvated proteins. The dielectrophoretic susceptibility for proteins is in the range of $10^4$, significantly exceeding traditional estimates limiting it to values below unity. Part of this large magnitude of the dielectrophoretic response is the cavity susceptibility of the protein-water interface, which significantly exceeds dielectric estimates. The study analyzes local fields inside the protein in terms of the reaction-field and directing-field components. We find that the local field exceeds the external field by a substantial factor described by the local field susceptibility. The electric field produced by water inside the protein is retarded by 3–4 orders of magnitude compared to the bulk.

# Introduction

Dielectrophoresis describes a set of phenomena related to manipulation of either charged or uncharged particles with the gradient of the electric field.[1,2] The dielectrophoretic force $\mathbf{f}_{\mathrm{DEP}}$ acting on a particle is proportional to the gradient of the field squared. The main challenge for measurements and theory is to determine the proportionality constant, the dielectrophoretic susceptibility $\chi_{\mathrm{DEP}}$

$$\mathbf{f}_{\mathrm{DEP}} = \epsilon_0 \chi_{\mathrm{DEP}} \nabla E^2 \tag{1}$$

where $\epsilon_0 \simeq 8.854 \times 10^{-12}$ (F/m) is the vacuum permittivity.

For a particle viewed as a dielectric object, there is no stationary dipole associated with it if the material is paraelectric. The dipole moment is induced by the field. In contrast, a ferroelectric domain carries an overall dipole moment, even though the domain dipoles can cancel out when randomly oriented in a macroscopic material. For a paraelectric material, that has no stationary dipole, the susceptibility $\chi_{\mathrm{DEP}}$ scales linearly with the volume of the particle or as the cube of its effective radius $R_0$

$$\chi_{\mathrm{DEP}} \propto R_0^3 \tag{2}$$

The dielectric properties of the particle enter the susceptibility through the electrostatic boundary-value problem[3] and are usually represented by the Clausius-Mossotti factor[1] (see below). The linear scaling with the volume can be understood by viewing the particle as a collection of $N$ individual dipoles, which can be aligned along the external field. The total induced dipole, which ultimately determines the overall force, is the sum of individual dipoles which are on average aligned along the field.

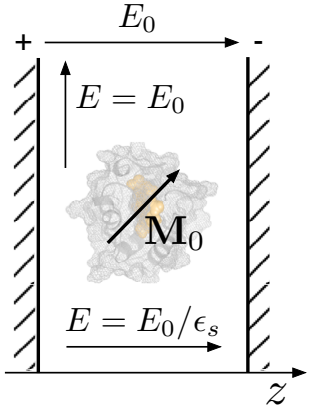


Figure 1: Schematic drawing of a protein in solution placed in the uniform field of a plane capacitor. The field of external charges at the plates of the capacitor is $E_0$ and the total (Maxwell) field inside the capacitor is $E$. The Maxwell field and the field of external charges are connected through the dielectric constant $E = E_0/\epsilon_s$, when the external field is applied perpendicular to the slab. The boundary conditions require $E = E_0$, when the external field is parallel to the slab, which typically applies to light absorption.

This line of thought, mostly used when considering particles on the micrometer length scale, needs modification when molecular objects are considered.[4] A molecule typically carries an asymmetric distribution of charge and can be assigned a permanent dipole moment. It can thus be viewed as a ferroelectric domain from the viewpoint of materials science. The narrow definition of dielectrophoresis as manipulation of nonpolar materials needs to be extended to include broadly defined nonionic particles. Permanent dipoles, that is dipolar particles, fall in this definition.

If the dipoles are allowed to orient randomly, one gets a zero average dipole moment $\langle \mathbf{M}_0 \rangle = 0$. When a nonuniform field is turned on at $t = 0$, there will be no force on an ensemble of dipoles given that the force is the product of the dipole moment with the field gradient.[3] The dipoles will, however, align on average with the field on the time-scale of each particle's rotation and the total force on an ensemble of dipoles placed in the field gradient will grow from zero initially to a nonzero value at $t \to \infty$. Assuming that the external field is applied along the $z$-axis of the laboratory frame (Figure 1), it will produce average dipoles $\langle M_{0z} \rangle_E \propto M_0^2 E$ scaling linearly with the field and proportional to the dipole squared (linear response, see below).[5] The interaction energy of polarized dipoles with the field, $\propto \langle M_{0z} \rangle_E E$, will be quadratic in the field and the force will have the form of eq 1. Importantly, the dielectrophoretic susceptibility gains quadratic scaling with the molecular dipole moment

$$\chi_{\mathrm{DEP}} \propto M_0^2 \tag{3}$$

The scaling with the volume from eq 2 does not need to be included in this limit. Further, the dipole moment scales linearly with the particle radius, $M_0 \propto R_0$, and the susceptibility of a dipolar particle scales as $R_0^2$. As the size of the particle grows, the cubic scaling in eq 2 becomes dominant and the permanent dipole can eventually be neglected for sufficiently large particles. The traditional view of dielectrophoretic susceptibility as originating from the collection of $N$ induced dipoles applies to this limit.[1]

Proteins do not fall in the limit of cubic scaling of eq 2. Of course, the molecular groups of

the protein carry electronic polarizability and can be viewed as a collection of many induced dipoles when placed in an external electric field. This induced-dipole component of $\chi_{\mathrm{DEP}}$ scales according to eq 2, as expected. However, the permanent dipole of a typical globular protein dominates over the dipoles induced due to electronic polarizability. Proteins are sufficiently asymmetric to produce dipole moments in the range of a few hundreds of debye units due to asymmetric distributions of charged residues exposed to water and charges of the N- and C-termini.[6,7] For these solutes, the quadratic scaling with the protein dipole moment dominates in the dielectrophoretic susceptibility and eq 3 applies.

The consequences of this perspective are discussed here in the light of new microsecond timescale molecular dynamics (MD) simulations of two globular proteins, ubiquitin and lysozyme. We show that dielectrophoretic susceptibility arising from aligning the dipole moments of these molecules with the field is many orders of magnitude higher than one would anticipate from the dielectric boundary-value solution leading to eq 2. We connect the dielectrophoretic susceptibility to dielectric measurements of protein solutions and show that our conclusions are supported by this technique. Direct measurements of the dielectrophoretic susceptibility are very challenging and have not been fully accomplished so far.[8,9] The connection between this property and dielectric spectroscopy of solutions offered here should provide a reliable access to this parameter as long as dielectrophoresis is dominated by the permanent dipole. We show in our analysis of atomistic simulations and experimental data that the influence of permanent protein dipoles on dielectrophoresis are considerably more relevant than other polarization effects that scale with the protein volume.

## Dielectrophoretic susceptibility

Consider a protein in solution placed between the plates of a plane capacitor (Figure 1). The external charges at the plates produce the external (vacuum) electric field $E_0$ along the axis $z$ perpendicular to the solution slab. The field $E_0 = \sigma_0/\epsilon_0$ is determined by the

surface density of free charges $\sigma_0$ at the capacitor plates. In contrast, the voltage on the capacitor plates $\phi$ specifies the Maxwell field $E = \phi/d$, where $d$ is the separation between the plates. The Maxwell field is a global field characterizing the entire dielectric.[3,10] It combines the field of external free charges on the conductors with the field of bound charges of the molecules of the dielectric material (including the surface charges). For the plane capacitor, these two fields are related by the static dielectric constant $\epsilon_s$: $E = E_0/\epsilon_s$. The Maxwell field is reduced compared to the vacuum field by the screening effect of the bound (molecular) charges.

Given that the Maxwell field is easily controlled in experiment and can be calculated by solving the dielectric boundary-value problem,[3] this field enters the dielectrophoretic force in eq 1. This simplicity is, however, not shared by statistical theories of dielectrics.[2,5] The issue here is that the interaction term entering the Hamiltonian of the dielectric in the field, $-M_z E_0$, is based on the vacuum field $E_0$ and the total dipole $M_z$ of the sample when the field is applied along the $z$-axis (Figure 1). The statistical theory has to be formulated in terms of the vacuum field $E_0$ since $E$ is a statistical average itself and cannot enter the Hamiltonian. This formulation allows one to consistently produce the required statistical averages, and it leads to the chemical potential of the protein in the external field[10,11]

$$\Delta\mu_0 = -\tfrac{1}{2}\langle M_{0z}\rangle_E E_0 \tag{4}$$

Here, $\langle M_{0z}\rangle_E$ is the average dipole moment of the protein and the surrounding hydration shell (interface dipole) induced by the applied field.

It is instructive to derive eq 4 from electrostatic arguments to contrast them with the standard statistical derivation. Consider a dielectric with $N_0$ solutes carrying dipole moments $\langle M_{0z}\rangle_E$ placed in the plane capacitor shown in Figure 1. Assume that the charges on the plates are fixed, which means that the dielectric displacement $D$ along the $z$-axis is constant.

The total free energy of the dielectric becomes[3,10]

$$\mathcal{F} = \tfrac{1}{2}\Omega DE = \tfrac{1}{2}\epsilon_0^{-1}\Omega D^2 - \tfrac{1}{2}M_z E_0 \tag{5}$$

where $\Omega$ is the volume occupied by the dielectric and $E_0 = D/\epsilon_0$ is the vacuum field. The first term on the right-hand side in this equation is the free energy of the vacuum electrostatic field and the second term is the free energy of polarizing the dielectric. The free energy of polarizing the solutes is obtained by separating their individual dipole moments

$$\Delta\mathcal{F}_0 = -\tfrac{1}{2}N_0\langle M_{0z}\rangle_E E_0 \tag{6}$$

The alteration of the chemical potential due to the applied field in eq 4 is the corresponding free energy change per solute.

To calculate the chemical potential of electric polarization, one needs a statistical definition of the average dipole moment $\langle M_{0z}\rangle_E$ in eq 4. The complete theory presented below involves two components of the induced dipole: the dipole induced by orienting the solute dipole and the dipole induced in the hydration shell. We will focus on the solute dipole for now to simplify the argument.

Many experimental applications, such as dielectric spectroscopy, employ weak electric fields allowing one to use the linear response approximation for calculating $\langle M_{0z}\rangle_E$. The condition of applying linear response is the smallness of $M_0E_0$ compared to the thermal energy $k_\mathrm{B}T$, which means $E < 1.2\times10^7/(\epsilon_s M_0)$ V/cm, where $M_0$ is in debye units. The average dipole aligned with the field becomes

$$\langle M_{0z}\rangle_E = \beta\langle M_{0z}M_z\rangle E_0 \tag{7}$$

where $\beta = (k_\mathrm{B}T)^{-1}$ is the inverse temperature and the statistical average $\langle\dots\rangle$ is taken over the dielectric sample with no field applied to it. It is important to stress that the statistical

average in eq 7 is taken over the product of the protein dipole $M_{0z}$ and the total dipole $M_z$ of the entire sample. If a spherical macroscopic region is chosen around the protein, which requires considering spherical water shells in the analysis of simulations, one can replace the product of two $z$-projections with one third of the scalar product, with the result for the chemical potential

$$\Delta\mu_0 = -\tfrac{1}{6}\beta\langle\mathbf{M}_0\cdot\mathbf{M}\rangle E_0^2 \tag{8}$$

The chemical potential change is next applied to determine the dielectrophoretic force. Moving particles in condensed media involves heat transfer (flow of entropy) thus making mechanical definitions of the dielectric forces inapplicable.[10,11] Instead, the force is produced by the gradient of the chemical potential at the constant temperature maintained between the subsystem and the thermal bath. Provided that the electric field $E_0$ changes on a length scale far exceeding linear dimensions of the protein, the gradient of the chemical potential in eq 8 leads to the dielectrophoretic force

$$\mathbf{f}_{\rm DEP} = \tfrac{1}{6}\beta\langle\mathbf{M}_0\cdot\mathbf{M}\rangle\nabla E_0^2 \tag{9}$$

There is a clear disconnect between eq 9 and eq 1 commonly used in the literature: the latter is expressed in terms of the gradient of the Maxwell field $E$, while eq 9 is given in terms of the external field $E_0$. Thermodynamics requires that the chemical potential $\mu_0 = \mu_0(T,P,D)$ is a function of dielectric displacement $D$,[11] which is fixed by the external charges. Therefore, once the charges on the device creating the field are fixed, that setup determines the vacuum field, the dielectric displacement, and the chemical potential of the solute in solution. The Maxwell field is the global field established in a dielectric device by manipulating the electrochemical potentials of conduction electrons in the conductors (the voltage on the plates). If the potential $\phi$ and the Maxwell field $E = \phi/d$ are varied at $t = 0$, this does not imply that the medium polarization is changed locally around the solute to affect its chemical potential at $t = 0$. Instead, the sample polarization changes on the time

scale of Debye relaxation of the solvent and changes in the Maxwell field reach solutes locally only when this relaxation has been completed.

These physical arguments make clear that the chemical potential must be a function of the vacuum field. The connection between $E$ and $E_0$ can be established from the known distribution of charge on the conductors, which follows from the solution of the boundary-value problem. Once this solution is established, the field of the free charges on the conductors provides $E_0$. This connection is not required for our purposes since we are only interested in the susceptibility entering the force as a linear transport coefficient. However, one can anticipate that in configurations similar to the plane capacitor the external field will be screened locally by the dielectric and one can adopt the capacitor configuration with $E_0 = \epsilon_s E$. With this assumption in place one can connect eqs 1 and 9. The common practice is to list not $\chi_{\mathrm{DEP}}$, which carries the units of the volume, but a unitless quantity $K$ according to the equation

$$\chi_{\mathrm{DEP}} = \tfrac{3}{2}\epsilon_s \Omega_0 K \tag{10}$$

where $\Omega_0 = (4\pi/3)R_0^3$ is the volume occupied by the solute with the effective radius $R_0$. One finally obtains for $K$

$$K_d = \frac{\epsilon_s \beta}{9\epsilon_0 \Omega_0} \langle \mathbf{M}_0 \cdot \mathbf{M} \rangle \tag{11}$$

where the subscript "d" specifies the dielectrophoretic susceptibility due to a permanent dipole.

Before addressing the parameters affecting $K_d$, we first make a short detour to the theory of dielectrics to introduce unitless parameters typically involved in theories of electric polarization.[5] The dielectric constant of a polar liquid $\epsilon_s$ is given by the Kirkwood-Onsager equation in terms of two parameters, the unitless density of dipoles $y$ and the Kirkwood dipolar correlation factor $g_K$

$$\frac{(\epsilon_s - 1)(2\epsilon_s + 1)}{9\epsilon_s} = g_K y \tag{12}$$

The parameter $y$ is given in terms of the molecular dipole moment $m$ and the number density

$\rho = N/\Omega$, where $N$ is the number of liquid dipoles placed in volume $\Omega$ occupied by the liquid

$$y = \beta m^2 \rho/(9\epsilon_0) \tag{13}$$

We discuss the extension of eq 12 to polarizable liquids below. The Kirkwood factor is defined equally for both nonpolarizable and polarizable liquids and is given by the average cosine between a target dipole $\hat{\mathbf{m}}_i$ in the liquid and all surrounding dipoles $\hat{\mathbf{m}}_j$

$$g_K = 1 + \sum_{j \neq i} \langle \hat{\mathbf{m}}_i \cdot \hat{\mathbf{m}}_j \rangle \tag{14}$$

where $\hat{\mathbf{m}}_i$ and $\hat{\mathbf{m}}_j$ are the unit vectors specifying dipolar orientations.

Following the analogy with bulk dielectrics, a static unitless dipolar density $y_0$ is introduced for the dipole moment $M_0$ of the protein

$$y_0 = \beta M_0^2/(9\epsilon_0 \Omega_0) \tag{15}$$

This notation is more convenient than an alternative use of the number density of solutes $\rho_0 = N_0/\Omega$, in analogy with $\rho$ in eq 13, because the dielectrophoretic response of a single protein molecule is usually considered. Given that the protein dipole scales as the size of the molecule, one anticipates that the parameter $y_0$ scales inversely with the protein size

$$y_0 \propto R_0^{-1} \propto M_p^{-1/3} \tag{16}$$

where $M_p$ is the molar mass of the protein. The importance of the parameter $y_0$ becomes immediately clear if one neglects the cross correlations between $\mathbf{M}_0$ and the surrounding medium and replaces $\mathbf{M}$ with $\mathbf{M}_0$ in eq 11. This leads to $K_d \propto y_0$.

The need to account for the cross-correlations between a selected dipole ($\mathbf{M}_0$ here) and the surrounding medium has remained a major challenge for all theories of dielectrics, which

has never been resolved in a satisfactory fashion. The appearance of the Kirkwood factor $g_K$ (eq 14) corresponds to selecting a single liquid dipole, and in that case too it remains a mostly unknown parameter of the theory.[12] In the case of a solute sufficiently large compared to the solvent, a mean-field account of the cross-correlations is achieved in terms of the cavity susceptibility $\chi_c$ which we discuss in significant detail below. When this correction factor is introduced, one arrives at the equation for the dielectrophoretic susceptibility of a dipole

$$K_d = \epsilon_s \chi_c y_0 \tag{17}$$

The cavity susceptibility $\chi_c$ in eq 17 is an important ingredient of the theory because the standard theories of dielectrics[5,13] predict a very low value for it. One obtains for a spherical solute

$$\chi_c^M = \frac{3}{2\epsilon_s + 1} \tag{18}$$

where the superscript "M" stands for Maxwell's electrostatics. This result appears from solving the dielectric boundary-value problem for a spherical void in a dielectric polarized by the external uniform field. In th3is form, $\chi_c$ would strongly suppress $K_d$ when used in eq 17. However, both the molecular dynamics (MD) simulations shown below and experimental data indicate that eq 18 does not provide a reliable estimate of $\chi_c$. Instead, one can use the direct correlation between the protein dipole $\mathbf{M}_0$ and the sample (solution) dipole $\mathbf{M}$

$$\chi_c = \langle \mathbf{M}_0 \cdot \mathbf{M} \rangle / \langle \mathbf{M}_0^2 \rangle \tag{19}$$

One assumes that both average dipoles are equal to zero; changes from the averages, e.g. $\delta\mathbf{M}_0 = \mathbf{M}_0 - \langle \mathbf{M}_0 \rangle$, are usually preferred in the analysis of numerical simulations with limited statistics. We show below that calculating dipolar cross correlations is equivalent, in the framework of dielectric theories, to solving the boundary-value problem leading to eq 18. This equality does not extend, however, to microscopic interfaces.

The correlation between the protein and sample dipoles contains the self variance $\langle \mathbf{M}_0^2 \rangle$ and the cross correlation $\langle \mathbf{M}_0 \cdot \mathbf{M}_w \rangle$ between the protein and water dipoles

$$\langle \mathbf{M}_0 \cdot \mathbf{M} \rangle = \langle \mathbf{M}_0^2 \rangle + \langle \mathbf{M}_0 \cdot \mathbf{M}_w \rangle \tag{20}$$

The idea of "screening" implies that this cross correlation is negative, thus reducing the self variance. The dielectric result in eq 18 in fact implies a nearly complete cancellation between the two terms in $\langle \mathbf{M}_0 \cdot \mathbf{M} \rangle$. It is easy to see that this prediction should be approached with caution given that the cavity susceptibility can be also viewed as the protein-water Kirkwood correlation factor.

If the permanent dipole moments of water and protein are $m_w$ and $M_0$, one can write (cf. to eq 14)

$$\chi_c = g_K^{0s} = 1 + \frac{m_w}{M_0} \sum_{j=1}^{N_w} \langle \hat{\mathbf{m}}_0 \cdot \hat{\mathbf{m}}_{wj} \rangle \tag{21}$$

where $\hat{\mathbf{m}}_0$ and $\hat{\mathbf{m}}_w$ are the protein and water unit vectors and the sum runs over all $N_w$ water molecules. Many polar liquids display Kirkwood factors close to unity[14,15] and one might anticipate that this result is shared by the protein-water interface. We indeed find this expectation to hold as discussed in detail below. The cross-correlations between the protein and water dipoles are multiplied by a small factor $m_w/M_0$, which scales as $\propto R_0^{-1}$ with the effective protein radius. However, the number of first-shell water molecules, which matter the most for the average cosines, scales as the protein surface $\propto R_0^2$. The overall result depends on the effective length of statistical correlations between the protein charges and surface waters. The final outcome might also be dictated by the protein shape. Depending on either prolate or oblate shape of the protein about the dipole axis, different numbers of water molecules can find themselves in predominantly parallel or antiparallel orientation in respect to the protein dipole. The range of $\chi_c$ values can potentially be broader than Kirkwood factors of bulk polar liquids.

The equations presented above determine the dielectrophoretic susceptibility dominated

by the permanent dipole of the solute. The solute dipole is not the only component of the overall polarization arising when the solute is polarized by the external field. An additional dipole $\mathbf{M}^{\text{int}}$ comes from the polarized solvation shell. The overall dipole associated with the solute becomes[4]

$$M_{0z} = \langle M_{0z} \rangle_E + \langle M_z^{\text{int}} \rangle_E \tag{22}$$

The need for the second component becomes clear if one considers the case of a zero solute dipole, $\mathbf{M}_0 = 0$. The dividing dielectric surface between the solute and the surrounding solvent is still polarized. In dielectric theories, the polarization of a spherical void by an external field leads to the dipole oriented opposite to the applied field[3,11]

$$\langle M_{0z}^{\text{int}} \rangle_E = -\frac{3\Omega_0}{2\epsilon_s + 1} P_z \tag{23}$$

where $P_z = \epsilon_0(1 - \epsilon_s^{-1})E_0$ is the polarization density of the uniformly polarized dielectric. By applying this dielectric result to the steps outlined above, one arrives at the Clausius-Mossotti form of the dielectrophoretic susceptibility

$$K_{\text{CM}} = -\frac{\epsilon_s - 1}{2\epsilon_s + 1} \tag{24}$$

The dielectrophoretic susceptibility is negative in this limit, meaning that the solute is repelled from the region of a higher electric field. If a bulk dielectric constant $\epsilon_p$ is assigned to the protein, $\epsilon_s$ has to be replaced by $\epsilon_s/\epsilon_p$ according to the standard rules of the dielectric boundary-value problem.[11] The resulting expression is commonly adopted to describe dielectrophorisis of large nonpolar solutes

$$K_{\text{CM}} = \frac{\epsilon_p - \epsilon_s}{\epsilon_p + 2\epsilon_s} \tag{25}$$

It is clear from this derivation that the standard Clausius-Mossotti form of the dielectrophoretic susceptibility can be viewed as the result of polarizing the protein-water divid-

ing surface by the external field. The resulting dielectric form limits the range of $K$ to $-0.5 \leq K_{\mathrm{CM}} \leq 1$. Such restrictions are eliminated when both the alignment of the permanent dipole, leading to $K_d$ (eq 17), and the interface polarization are combined in the total dipole associated with the polarized solute. This problem is more complex than the standard Clausius-Mossotti solution since the interface is now polarized by both the solute dipole and the external field. The solution of the problem is achieved by introducing the interface susceptibility $\chi^{\mathrm{int}}$

$$\langle M_z^{\mathrm{int}} \rangle_E = \epsilon_0 \chi^{\mathrm{int}} \Omega_0 E_0 \tag{26}$$

It turns out[4] that no new susceptibility is required and $\chi^{\mathrm{int}}$ can be expressed in terms of the cavity susceptibility $\chi_c$. Specifically, $\chi^{\mathrm{int}}$ can be related to the deviation of the cavity susceptibility from the result known as the virtual Lorentz cavity,[13] which leads to the following form for a spherical sample

$$\chi_c^L = \frac{\epsilon_s + 2}{3\epsilon_s} \tag{27}$$

The connection between the cavity susceptibility $\chi_c$ and the interface susceptibility $\chi^{\mathrm{int}}$ is given by the following relation (see eq S22 in SI for derivation)

$$\chi^{\mathrm{int}} = \frac{9}{2(\epsilon_s - 1)} \left( \chi_c - \chi_c^L \right) \tag{28}$$

Combined together, these results lead to a universal form for the dielectrophoretic susceptibility incorporating both the effect of the solute permanent dipole and the interface polarization[4]

$$K = \epsilon_s \chi_c y_0 + \frac{3\epsilon_s}{2(\epsilon_s - 1)} \left( \chi_c - \chi_c^L \right) \tag{29}$$

The virtual cavity construct introduced by Lorentz does not anticipate the formation of surface charge at the dividing surface separating the solute from the surrounding polar medium. Hydrophobic solutes, for which the interfacial water dipoles align mostly parallel

to the dividing surface,[16] provide a physical realization of the Lorentz virtual cavity.[17] It is easy to see that putting $y_0 = 0$ in eq 29 is not sufficient to recover the Clausius-Mossotti limit. One needs to additionally adopt the rules of Maxwell's electrostatics for the boundary conditions and the corresponding surface-charge density. Those lead to $\chi_c = \chi_c^M$ (eq 18) and the recovery of the Clausius-Mossotti result in eqs 24 and 25. This is the limit of eq 2 when the dielectrophoretic susceptibility scales linearly with the protein volume. In the opposite limit of $y_0 \gg 1$, the first term dominates in eq 29 and one gets $K \to K_d$ (eq 15). It is important to stress that the solute volume cancels out from the dielectrophoretic susceptibility $\chi_{\rm DEP}$ when the expression for $K_d \propto y_0 \propto \Omega_0^{-1}$ is substituted to eq 10. One obtains the quadratic scaling with the solute dipole (eq 3)

$$\chi_{\rm DEP} \simeq \epsilon_s^2 \chi_c \beta M_0^2/(6\epsilon_0) \simeq 50.6 \epsilon_s^2 \chi_c M_0^2 \ \text{Å}^3 \tag{30}$$

where in the last equation $T = 300$ K and $M_0$ is in debye units. This equation neglects fluctuations of the dipole moment caused by conformational flexibility (see below).

The discussion so far has focused on a spherical dipolar or nondipolar solute placed in the polarizable medium with the solute-solvent interface polarized either by the rules of Maxwell electrostatics or by some more general rules specific to the interface of a polar liquid with a molecular solute. These unspecified non-Maxwellian rules are integrated into the cavity susceptibility $\chi_c$ which needs to be determined either from numerical simulations, from microscopic solvation theories, or from experimental observables. We now turn from the model spherical solute to proteins in TIP3P water sampled by MD simulations. Our focus is on the electric field of the water shell inside the protein with and without a weak external field applied to the solution.

# Fields inside the protein

The electric field inside the protein needs to be separated into distinct components to address the interaction energy of the protein dipole with the external field and the torque rotating the dipole to align it with the field. Even in the absence of an external field, thermal agitation of the hydration shell leads to a fluctuating microscopic electric field $\mathbf{E}_s$. This field fluctuates around some average value consistent with the charge distribution of the protein. To understand its origin, one can proceed from the multipolar expansion of the protein charge.

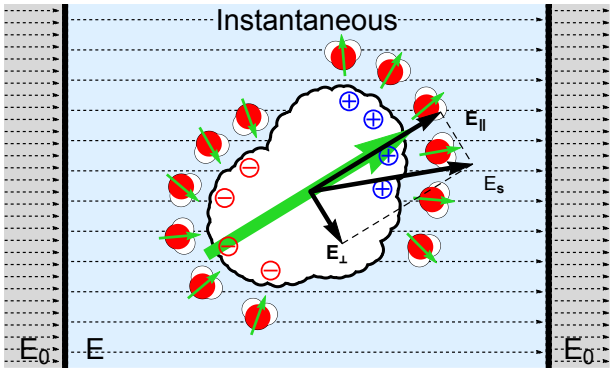


Figure 2: Projections of the solvent field for a random instantaneous configuration of the protein. The green arrow indicates dipole moments of the protein (large arrow) and of the water molecules (small arrows). The random motion of the water dipoles is responsible for the fluctuating solvent field $\mathbf{E}_s$, which is separated into projections parallel, $\mathbf{E}_\parallel$, and perpendicular, $\mathbf{E}_\perp$, to the protein dipole.

The total charge of the protein, placed at the center of charge, induces a constant solvent electrostatic potential in an effective spherical cavity representing the protein's repulsive core. No field comes from this component. The next multipole, the protein dipole, polarizes the solvent and induces a field parallel to the dipole, $\mathbf{E}_\parallel = \hat{\mathbf{m}}_0(\hat{\mathbf{m}}_0 \cdot \mathbf{E}_s)$, $\hat{\mathbf{m}}_0 = \mathbf{M}_0/M_0$ (Figure 2). Averaged over the water configurations, this field becomes the Onsager reaction field[13]

$$E_r = \langle \hat{\mathbf{m}}_0 \cdot \mathbf{E}_s \rangle \tag{31}$$

If the response is linear, the magnitude of the reaction field is proportional to the magnitude

of the solute dipole, with the reaction-field susceptibility $g_r$ as the proportionality coefficient

$$E_r = g_r M_0 \tag{32}$$

Dielectric theories calculate $g_r$ by solving the boundary-value problem. One gets a closed-form expression for a spherical solute with the radius $R_0$

$$g_r = \frac{1}{4\pi\epsilon_0 R_0^3}\frac{2(\epsilon_s - 1)}{2\epsilon_s + 1} \tag{33}$$

We do not use this approximate solution here and, instead, calculate the reaction field from MD configurations applied to eq 31.

The projection of the solvent field on the solute dipole moment makes zero torque and cannot rotate the dipole. It is the projection of the solvent field perpendicular to the protein dipole, $\mathbf{E}_\perp = \mathbf{E}_s - \hat{\mathbf{m}}_0(\hat{\mathbf{m}}_0 \cdot \mathbf{E}_s)$, that is responsible for the torque producing random rotations of the dipole moment[18] (Figure 2). The average of this projection, $E_d = \langle \mathbf{E}_\perp \rangle$, is the directing field originally introduced by Onsager.[13,19] The directing field averages out to zero in the absence of an external field when the charge distribution of the solute is represented by the dipole

$$E_d = 0 \tag{34}$$

The average solute field $\langle \mathbf{E}_s \rangle$ is also zero in this case. For the analysis of simulations, $\langle \mathbf{E}_s \rangle$ is subtracted from $\mathbf{E}_s$ and only fluctuations around the average are considered.

When a weak field along the $z$-direction perpendicular to the solution slab (Figure 1) is applied to the solution, a small fraction of the protein and water dipoles align with the field thus creating an observable polarization of the solution. Most of the proteins and water molecules continue almost unaffected random motion, and their dynamics are not altered by the external field when linear response is applied. The average solvent field $\langle \mathbf{E}_s \rangle_E$ in the presence of $E_0$ becomes nonzero because proteins aligned with the field also polarize

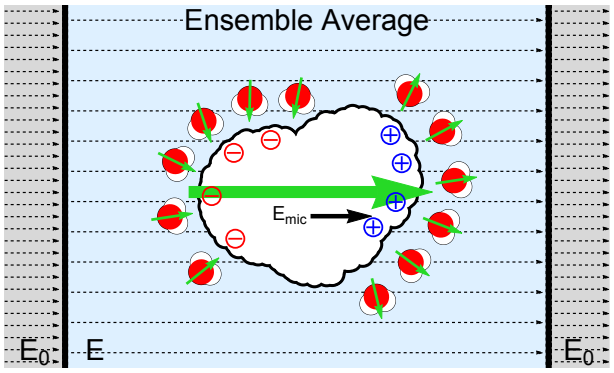


Figure 3: Ensemble-average configuration of the protein in an external field. The average reaction field $R$ and the directing field $E_D$ add up to the microscopic field of the solvent $E_{\mathrm{mic}}$.

their water shells (Figure 3). This average field, which we call the microscopic field $E_{\mathrm{mic}}$ to distinguish it from other components, is easily found from perturbation theory

$$E_{\mathrm{mic}} = \langle E_s^z \rangle_E = \beta \langle E_s^z M_z \rangle E_0 = \tfrac{1}{3}\beta \langle \mathbf{E}_s \cdot \mathbf{M} \rangle E_0 \tag{35}$$

where isotropy of the sample is applied in the last step given that the average $\langle \dots \rangle$ refers to no field. This assumed isotropy requires to use spherical samples in the simulations aimed at producing the corresponding averages. Further, the microscopic field is also a sum of the average field $E_R = \langle \mathbf{E}_{\parallel} \rangle_E$ always aligned with the protein dipole and the average perpendicular component $E_D = \langle \mathbf{E}_{\perp} \rangle_E$ responsible for a nonzero net directing field $E_D$

$$E_{\mathrm{mic}} = E_R + E_D = (\chi_R + \chi_D)\, E_0 \tag{36}$$

where $\chi_R = E_R/E_0$ and $\chi_D = E_D/E_0$ are the corresponding susceptibilities (we use upper case subscripts to distinguish averages in the presence of the external field). The total field inside the protein, which we call the local field $E_{\mathrm{loc}} = E_0 + E_{\mathrm{mic}}$, is a sum of the external field $E_0$ and the average solvent field $E_{\mathrm{mic}}$. The corresponding linear susceptibility becomes

$$\chi_{\mathrm{loc}} = 1 + \chi_R + \chi_D \tag{37}$$

The reaction field established along the protein dipoles aligned on average with the external field is obtained by taking the statistical average of $\mathbf{E}_{\|} = \hat{\mathbf{m}}_0(\hat{\mathbf{m}}_0 \cdot \mathbf{E}_s)$. The linear susceptibility becomes

$$\chi_R = \tfrac{1}{3}\beta\langle(\mathbf{E}_s \cdot \hat{\mathbf{m}}_0)(\hat{\mathbf{m}}_0 \cdot \mathbf{M})\rangle \tag{38}$$

where, similarly to eq 35, the assumption of an isotropic sample when no external field is applied accounts for the factor of 1/3. The directing field $E_D$ in eq 36 is found by subtracting the reaction field $E_R$ from the microscopic field $E_{\mathrm{mic}}$. Onsager applied the assumption of equality between the directing and cavity susceptibilities, $\chi_D = \chi_c$, in his mean-field theory of dielectrics.[19] As we show below, these susceptibilities are indeed equal in dielectric theories. They do not have to coincide, but turn out to be close in magnitude for bulk polar liquids.[20] This expectation is, however, not realized for the susceptibilities of proteins calculated from MD simulations (see below).

Based on the reaction-field susceptibility $g_r$ (eq 32), one can seek a mean-field solution for the induced reaction field $E_R = \chi_R E_0$ in eq 38. If one assumes that the projection of $\mathbf{E}_s$ on the protein dipole is mostly induced by the dipole itself, one can put $\hat{\mathbf{m}}_0(\hat{\mathbf{m}}_0 \cdot \mathbf{E}_s) = 2g_r\hat{\mathbf{m}}_0$ in eq 38 with the result

$$\chi_c^{\mathrm{MF}} = \frac{3\chi_R}{\beta M_0 E_r} \tag{39}$$

where eq 19 was used for the cavity-field susceptibility $\chi_c$. Further, the susceptibility $\chi_R$ is calculated from eq 38 and $E_r$ is from eq 31. This equation provides a mean-field estimate of $\chi_c$ from the properties directly accessible from MD simulations. Its application to finite-size simulations requires corrections arising from constraining the volume of water around the protein as discussed below. These corrections apply to both the mean-field result (eq 39) and to direct calculations of the cavity susceptibility from dipolar correlations (eq 19).

In contrast to the field components discussed here, the cavity-field susceptibility does not account for any physical field in the context of a solute carrying distributed molecular charge. The cavity field susceptibility appears as an attempt to confine the action of the

external field to a single dipole, the dipole moment of the protein in the present context. As we showed above $\chi_c$ appears as the correction in replacing $\langle \mathbf{M}_0 \cdot \mathbf{M} \rangle$ by $\langle \mathbf{M}_0^2 \rangle$ in linear perturbation theories. In contrast, the physical cavity field $E_C$ accounting for the same effect is obtained by a virtual process of removing the solute dipole while preserving the interfacial structure. This thought experiment, which can be a reasonable reflection of reality in a solid dielectric, obviously cannot be achieved in any realistic situation of a solute carrying distributed atomic charges and placed in a liquid solvent (the interfacial structure changes when the dipole is removed). Only nonpolar solutes can be used as physical models to study the cavity field and to get direct access to the cavity-field susceptibility.[17] Little is known about this parameter beyond standard dielectric theories and such model calculations. Here, we calculate this parameter from MD simulations in terms of dipolar correlations (eq 19) and attempt to estimate its value from experimental data for protein solutions. The direct simulation route has the disadvantage of slow convergence as a function of the size of the spherical region chosen around the protein. This difficulty is the reason for suggesting eq 39 as an alternative approximate algorithm. Its performance is analyzed below.

# Dielectric spectroscopy of solutions

Connecting the dielectrophoretic susceptibility to dielectric experiment requires an equation for the dielectric constant of the mixture. The arguments used to derive the Kirkwood-Onsager equation[21,22] are applied here for an ideal solution containing $N_0$ proteins (the protein-protein Kirkwood factor is set to unity).

The Kirkwood-Onsager equation 8 and all following equations have been considered for the special case of nonpolarizable liquids suitable for comparison with simulations employing nonpolarizable force fields. For applications to dielectric measurements, the polar solvent has to be viewed as electronically polarizable. This implies that in addition to the static dielectric constant, the squared refractive index $\epsilon_\infty = n_D^2$ has to be included to account

for screening of electrostatic interactions by induced dipoles. To account for the electronic polarizability in the derivation of the Kirkwood-Onsager equation for mixtures, one can apply Frohlich's approach of viewing the permanent dipoles immersed in the continuum of electronic polarization characterized by $\epsilon_\infty$. To avoid dielectric discontinuities arising from the electronic polarization when applying an external field to the dielectric slab, one can view the surrounding medium as carrying the dielectric constant $\epsilon_\infty$. Only the surface polarization arising from the permanent dipoles in the slab will contribute to the boundary conditions. In this setup, the equation for the dielectric constant is derived by applying the external field $E_0$ first perpendicular to the slab and then parallel to it.[21]

When the electric field is applied perpendicular to the solution slab, the Maxwell field inside the slab is defined by the boundary conditions $E = E_0(\epsilon_\infty/\epsilon_{\rm mix})$ (Figure 1). The polarization of the solution with the dielectric constant $\epsilon_{\rm mix}$ follows from the standard steps of perturbation theory[13]

$$(\epsilon_{\rm mix} - \epsilon_\infty)\frac{\epsilon_\infty}{\epsilon_{\rm mix}}E_0 = \frac{\beta}{\epsilon_0\Omega}\langle M_z^2\rangle E_0 \tag{40}$$

where the dipole moment of the sample now includes $N_0$ protein molecules

$$\mathbf{M} = \sum_{i=1}^{N_0}\mathbf{M}_{0i} + \mathbf{M}_w \tag{41}$$

When, alternatively, the field is applied parallel to the plane of the slab, the boundary condition is $E = E_0$ and the response becomes

$$(\epsilon_{\rm mix} - \epsilon_\infty)E_0 = \frac{\beta}{\epsilon_0\Omega}\langle M_x^2\rangle E_0 \tag{42}$$

By multiplying this equation by the factor of two and adding to eq 40, one obtains the total dipole moment of the sample $\mathbf{M}^2 = M_z^2 + 2M_x^2$ ($x$ and $y$ directions are equivalent), which is independent of the shape of the sample and the orientation of the laboratory coordinate

frame. The result is the Kirkwood-Frohlich equation for mixtures

$$\frac{(\epsilon_{\rm mix}-\epsilon_\infty)(2\epsilon_{\rm mix}+\epsilon_\infty)}{9\epsilon_{\rm mix}} = (1-\eta_0)\frac{(\epsilon_s-\epsilon_\infty)(2\epsilon_s+\epsilon_\infty)}{9\epsilon_s} + \eta_0 y_0(2\chi_c - 1) \tag{43}$$

where $\eta_0 = N_0\Omega_0/V\Omega$ is the volume fraction of proteins in solution and eq 19 was used to account for cross correlations between the protein and water dipole moments. If the steps of the derivation are repeated for the bulk liquid, one obtains the standard form of the Kirkwood-Frohlich equation (cf. to eq 8)

$$\frac{(\epsilon_s-\epsilon_\infty)(2\epsilon_s+\epsilon_\infty)}{9\epsilon_s} = g_K y' \tag{44}$$

The new density of permanent dipoles $y'$ is based on the condensed-phase dipole moment $m'$ in contrast to the vacuum dipole $m$ in eq 9

$$y' = \beta(m')^2\rho/(9\epsilon_0). \tag{45}$$

The dipole moment $m'$ is enhanced compared to $m$ because of molecular polarizability.[19] The Onsager approximation for $m'$ assumes $m' = m(\epsilon_\infty + 2)/3$.

For the typical situation of $\epsilon_{\rm mix}, \epsilon_s \gg 1$, eq 43 can be rewritten as

$$\Delta\epsilon_{\rm mix}(\omega) = (9/2)\eta_0 y_0(\omega) + 9\eta_0 y_0(\omega)(\chi_c(\omega) - 1) + (1-\eta_0)\Delta\epsilon_w(\omega) \tag{46}$$

where we have introduced the frequency dependence of the dielectric functions and of the cavity susceptibility and put $\Delta\epsilon_{\rm mix}(\omega) = \epsilon_{\rm mix}(\omega) - \epsilon_\infty$ and $\Delta\epsilon_w(\omega) = \epsilon(\omega) - \epsilon_\infty$. The reason for eq 46 to be written in this form is that it represents three relaxation processes when they are separable by the corresponding relaxation times. The first term in eq 46 is $\beta$-relaxation produced by protein tumbling. The relevant time-scale $\tau_r$ of protein dipolar relaxation is

included in the Debye relaxation function[23] $y_0(\omega)$ replacing $y_0$ in the static limit (eq 15)

$$y_0(\omega) = y_0 \left(1 - i\omega\tau_r\right)^{-1} \tag{47}$$

Further, the last term in eq 46 is the $\gamma$-relaxation of bulk water reduced by $1 - \eta_0$ through the volume expelled by the proteins in solution.[24] The term in between, which is typically observed at frequencies $\sim 100$ MHz[6,25–27] intermediate between $\beta$- and $\gamma$-relaxation, is called the $\delta$-relaxation. Its origin, which is still disputed, has been attributed to either the protein-bound water[6,7,25] or to cross correlations between the protein and water dipoles.[28–30] This term appears, however, naturally from the exact Kirkwood-Onsager equation as a cross-correlation component, and we tentatively adopt this physical meaning for it. Note that the second term in eq 46 is zero if $\chi_c = 1$. This means no correlations between the protein dipole and its water shell (eqs 19 and 20). Written in terms of dipole moments of the protein and water, the $\delta$-relaxation term in eq 46 becomes

$$9\eta_0 y_0(\chi_c - 1) = \eta_0 \frac{\beta\langle \mathbf{M}_0 \cdot \mathbf{M}_w \rangle}{\epsilon_0 \Omega_0} \tag{48}$$

If a Debye relaxation process is assigned to each term in eq 46, one can assign the dielectric strengths $\Delta\epsilon_\beta$ and $\Delta\epsilon_\delta$ to two first terms

$$\begin{aligned} \Delta\epsilon_\beta &= (9/2)\eta_0 y_0 \\ \Delta\epsilon_\delta &= 9\eta_0 y_0(\chi_c - 1) \end{aligned} \tag{49}$$

The second relation implies that $\Delta\epsilon_\delta \propto y_0$ and, according to eq 16, this dielectric strength should scale with the protein molecular mass as $\propto M_p^{-1/3}$ at $\eta_0 \simeq$ Const.[26] The cavity susceptibility is nearly constant among proteins and does not strongly affect this dependence (see below). The combination of two dielectric strengths in eq 49 provides access to the cavity

susceptibility

$$\chi_c = 1 + \frac{\Delta\epsilon_\delta}{2\Delta\epsilon_\beta} \tag{50}$$

This equation predicts that the ability to observe $\delta$-dispersion is bound to the condition of $\chi_c > 1$, i.e., positive protein-water dipolar cross-correlations. If these correlations are negative, as the standard Maxwell equation (eq 18) would predict, the $\delta$-process should contribute a negative dielectric strength to the spectrum.

One can use an alternative route to the cavity susceptibility by rewriting eq 46 as follows

$$\frac{\Delta\epsilon(\omega)}{\eta_0} + \Delta\epsilon_w(\omega) = \frac{9}{2} y_0(\omega)(2\chi_c(\omega) - 1) \tag{51}$$

where

$$\Delta\epsilon(\omega) = \epsilon_{\mathrm{mix}}(\omega) - \epsilon(\omega) \tag{52}$$

is the dielectric function increment of solution over bulk water. This is the dielectric mixture formula for the solution of noninteracting proteins. At small concentrations of the protein, $\Delta\epsilon/\eta_0 \gg \Delta\epsilon_w$ and one gets a convenient practical relation

$$\Delta\epsilon(\omega) \simeq (9/2)\eta_0 y_0(\omega)(2\chi_c(\omega) - 1) \tag{53}$$

# Frequency-dependent dielectrophoresis

Like any linear susceptibility,[2,23,33] the dielectric susceptibility gains a dependence on frequency when oscillatory external fields are applied. As already discussed, both the dielectric constant $\epsilon_s$ and the unitless parameter $y_0$ (eq 15) become frequency-dependent functions, $\epsilon(\omega)$ and $y_0(\omega)$, respectively. The parameter $y_0(\omega)$ describes the extent of alignment of the protein dipole along the external field oscillating with the circular frequency $\omega$. When oscillations of the external field are faster than dipolar relaxation, the permanent dipole does

**Table 1: Results of MD simulations and the analysis of dielectric data.**

| Protein | $K^a$ | $K^b$ | $\chi_c^c$ | $\chi_c^d$ | $M_{\rm rms}^e$ | $R^f$ | $y_0$ | $\tau_0$, ns$^g$ |
|---|---|---|---|---|---|---|---|---|
| Ubiquitin$^h$ | 5709 | 8354[30] | 0.36 | 1.08 | 221 | 13.7 | 154 | 3.80 |
| | | | | | 238 | 13.7 | 178 | 4.34 |
| Lysozyme | 1691$^k$ | 3751[31] | 0.37 | 1.20 | 148 | 15.9 | 44 | 6.86 |
| Cytochrome $c^l$ | 6320 | 6643[9] | 0.54 | 1.09 | 238 | 18.7 | 67 | 12.8 |

[a]Results from 1 microsecond MD simulations. [b]Experimental estimates from dielectric measurements estimated from eq 60. [c]From MD simulations with the Lorentz correction factor for the spherical cutoff, eq 69. [d]From experimental data presented in Figure 5. [e]RMS dipole moment (D) of the protein estimates as $M_{\rm rms} = \sqrt{\langle \mathbf{M}_0^2 \rangle}$. [f]Radius of the protein in Å. [g]Exponential relaxation time of the time correlation function of the protein dipole moment. [h]The first line refers to 1 microsecond MD simulations without electrolyte ions in a large simulation box and the second line is for a 10 microsecond MD simulation with a 0.15 M electrolyte concentration (1:1 NaCl:KCl) in a minimal simulation box. [k]The value $K \simeq 1600$ was reported from MD simulations in ref 4. [l]From MD simulations at 310 K.[32]

not have sufficient time to align with the field and $y_0(\omega)$ decreases. The Debye form of the function $y_0(\omega)$ in eq 47 describes this dynamical freezing on the time scale of observation.

The dynamic cavity susceptibility $\chi_c(\omega)$ becomes a ratio of two dynamic correlation functions, both involving correlations of dipole moments, but scaled with the inverse temperature and the protein volume to produce dimensionless functions consistent with $y_0(\omega)$. These functions are

$$\chi(\omega) = \beta \langle \mathbf{M}_0 \cdot \mathbf{M} \rangle / (3\epsilon_0 \Omega_0) \left[ 1 + i\omega \tilde{\Phi}(\omega) \right] \tag{54}$$

and

$$\chi_0(\omega) = \beta \langle \mathbf{M}_0^2 \rangle / (3\epsilon_0 \Omega_0) \left[ 1 + i\omega \tilde{\Phi}_0(\omega) \right] \tag{55}$$

Here, the functions $\tilde{\Phi}(\omega)$ and $\tilde{\Phi}_0(\omega)$ are Fourier-Laplace transforms[33] of corresponding normalized time correlation functions. For instance, one has for $\tilde{\Phi}(\omega)$

$$\Phi(t) = \left[ \langle \mathbf{M}_0 \cdot \mathbf{M} \rangle \right]^{-1} \langle \mathbf{M}_0(t) \cdot \mathbf{M}(0) \rangle \tag{56}$$

and

$$\tilde{\Phi}(\omega) = \int_0^\infty dt \Phi(t) e^{i\omega t} \tag{57}$$

In the case of one-exponential decay, one obtains Debye relaxation in both cases with the relaxation times $\tau_M$ (eq 54) and $\tau_0$ (eq 55). From MD simulations discussed in more detail below, we indeed find mostly single-exponential relaxation with $\tau_M \approx \tau_0$. This result implies that the dynamic cavity susceptibility

$$\chi_c(\omega) = \chi(\omega)/\chi_0(\omega) \tag{58}$$

is nearly constant and is mostly determined by its static limit.

Dielectrophoresis dominated by the protein dipole moment, $y_0 \gg 1$ (Table 1), can be related to the dielectric increment of solutions. A connection between $K_d(\omega)$ and $\Delta\epsilon(\omega)$ of solution over bulk water leads to the following relation

$$K(\omega) = \frac{2}{9}\epsilon(\omega)\left(\frac{\Delta\epsilon(\omega)}{\eta_0} + \Delta\epsilon_w(\omega)\right)\frac{\chi_c(\omega)}{2\chi_c(\omega)-1} \tag{59}$$

The estimates of $\chi_c$ discussed below indicate that the term $\chi_c/(2\chi_c - 1)$ is close to unity and can be dropped in practical applications. One arrives at a practical equation

$$K(\omega) = \frac{2}{9}\epsilon(\omega)\left(\Delta\epsilon(\omega)/\eta_0 + \Delta\epsilon_w(\omega)\right) \tag{60}$$

This equation is further simplified at very small concentrations, $\eta_0 \to 0$, when the second term in the brackets can be dropped.

# Simulation Protocol

Equation 19 establishes the cavity susceptibility in terms of the cross-correlation between the protein dipole $\mathbf{M}_0$ and the total dipole of the macroscopic sample $\mathbf{M}$. When this equation is applied to simulation trajectories, the total dipole moment $\mathbf{M}_t = \mathbf{M}_0 + \mathbf{M}_w$ is calculated within a sphere with the cutoff radius $r_c$ drawn around the protein. One, therefore, needs

to incorporate corrections for excluding the macroscopic dipole $\mathbf{M}_{\text{out}}$ outside of the cutoff sphere. The outside dielectric is polarized by the dipole $\mathbf{M}_t$ at each configuration along the simulation trajectory. It turns out that this polarization results in a correction term independent of the radius $r_c$, which needs to be included independently of the size of the simulation box. This conclusion was reached previously.[17] The corresponding formalism is adopted here for calculating cross correlations between the dipole moments. The full derivation is given in the Supporting Information (SI), here we briefly outline the main steps.

The spherical cutoff leads to an additional susceptibility arising from the dipole moment $\mathbf{M}_{\text{out}}$ of the surrounding dielectric medium

$$\chi_c = \langle \mathbf{M}_0 \cdot \mathbf{M}_t \rangle / \langle \mathbf{M}_0^2 \rangle + \chi_{\text{out}} \tag{61}$$

The additional susceptibility is calculated here in the formalism of reciprocal-space susceptibility functions.[34] This approach formulates the linear inhomogeneous susceptibility of the solvent in the presence of a spherical solute excluding the polar liquid from its volume

$$\boldsymbol{\chi}(\mathbf{k}_1, \mathbf{k}_2) = \boldsymbol{\chi}_s(\mathbf{k}) \delta_{\mathbf{k}_1, \mathbf{k}_2} - \alpha \boldsymbol{\chi}_0(\mathbf{k}_1, \mathbf{k}_2) \tag{62}$$

The susceptibilities $\boldsymbol{\chi}_s$ and $\boldsymbol{\chi}_0$ here are second-rank tensors which are given in terms of scalar longitudinal and transverse projection functions. The first component, $\boldsymbol{\chi}_s$, is the dipolar microscopic susceptibility of the bulk usually given in terms of the orientational structure factors describing orientational correlations of the liquid dipoles.[33,34] The second summand, $\boldsymbol{\chi}_0$, is the alteration of the bulk susceptibility caused by the repulsive core of the solute. This component is multiplied with the scaling factor $\alpha$ switching between the physical dielectric interface possessing the surface charge ($\alpha = 1$) and the mathematical geometric separation of a virtual Lorentz cavity ($\alpha = 0$), which does not induce an interfacial restructuring of the medium dipoles.[4]

For the problem considered here, the spherical volume with the cutoff radius $r_c$ plays the role of a virtual solute carrying the dipole moment $\mathbf{M}_t$ and polarizing the medium outside of the cutoff. The electric field in reciprocal space is given as the product of the dipole moment and the reciprocal-space (second-rank) dipolar tensor $\tilde{\mathbf{T}}$

$$\tilde{\mathbf{E}}_0 = \tilde{\mathbf{T}} \cdot \mathbf{M}_t \tag{63}$$

Given this external field, the polarization of the medium outside of the cutoff is given as

$$\tilde{\mathbf{P}}(\mathbf{k}_1) = \int \frac{d\mathbf{k}_2}{(2\pi)^3} \boldsymbol{\chi}(\mathbf{k}_1, \mathbf{k}_2) \cdot \tilde{\mathbf{E}}_0(\mathbf{k}_2) \tag{64}$$

The polarization of the liquid outside of the spherical volume carrying the dipole moment $\mathbf{M}_t$ is produced through the dipolar tensor $\tilde{\mathbf{T}}$ in eq 63. If the spherical volume is taken from a macroscopic sample, the spatial Fourier transform of the dipolar tensor with a spherical cutoff is given by the following expression[35]

$$\tilde{\mathbf{T}} = -\frac{j_1(kr_c)}{\epsilon_0 k r_c} \left[ 3\hat{\mathbf{k}}\hat{\mathbf{k}} - \hat{\mathbf{1}} \right] \tag{65}$$

where $j_n(x)$ is the spherical Bessel function of order $n$[36] and $\hat{\mathbf{k}} = \mathbf{k}/k$ is the unit vector. This form for the dipolar tensor applies regardless of whether the interface with the surrounding medium is physical (Maxwell) of virtual (Lorentz). If, on the contrary, the spherical region polarizes the lattice of replicas of the simulation box considered in simulation protocols with periodic boundary conditions and Ewald sums used to calculate long-range electrostatics, one applies the Ewald dipolar tensor $\tilde{\mathbf{T}}_E$ listed by Neumann[35] and reproduced in the SI. The formalism outlined by eqs 62 and 64 is implemented with the dipolar tensor $\tilde{\mathbf{T}}$ for an infinite sample and tensor $\tilde{\mathbf{T}}_E$ for the simulation setup.

The cavity susceptibility is derived in SI

$$\chi_c = \chi_c(\alpha)\langle \mathbf{M}_0 \cdot \mathbf{M}_t \rangle / \langle \mathbf{M}_0^2 \rangle \tag{66}$$

In this expression, the dipole moment of the protein $\mathbf{M}_0$ is correlated with the dipole moment of the spherical region $\mathbf{M}_t$. If an infinite sample is polarized by $\mathbf{M}_t$, one finds the correction factor

$$\chi_c(\alpha) = \frac{\epsilon_s + 2}{3\epsilon_s} - \alpha \frac{2(\epsilon_s - 1)^2}{3\epsilon_s(2\epsilon_s + 1)} \tag{67}$$

The first term in this equation is the Lorentz cavity field assuming that the dividing surface between the inside and outside regions does not introduce a real physical interface (cf. to eq 27). In contrast, the limit $\alpha = 1$ describes a physical interface, when the dielectric boundary conditions of Maxwell's electrostatics apply. Taking this limit and combining the first two terms in eq 67 leads to the Maxwell dielectric cavity factor $\chi_c(\alpha = 1) = \chi_c^M$ given by eq 18.

For the periodic boundary conditions implementing Ewald formalism, switching from $\tilde{\mathbf{T}}$ to $\tilde{\mathbf{T}}_E$ replaces $\chi_c(\alpha)$ in eq 67 with $\chi_c(\alpha) + \alpha\chi_{\text{corr}}$ (see SI), where the correction terms is

$$\chi_{\text{corr}} = \frac{2(\epsilon_s - 1)^2}{3\epsilon_s(2\epsilon_s + 1)} \left[ \text{erfc}(\kappa r_c) + \frac{2\kappa r_c}{\sqrt{\pi}} e^{-(\kappa r_c)^2} \right] \tag{68}$$

Here, $\kappa$ is the direct-space screening parameter employed in Ewald sums[37] and $\text{erfc}(x)$ is the complimentary error function.[36] This correction term can be neglected for typical parameters employed in simulations of proteins and it is not considered in our calculations.

The derivation presented here clearly shows that cross correlations between the dipole within a spherical region with the outside polarized medium yield the result equivalent to solving the dielectric boundary-value problem for an empty cavity polarized by the external field[3] as long as discontinuity of the dielectric constant is assumed at the dividing surface ($\alpha = 1$). No such physical discontinuity is realized when a spherical region within the cutoff radius $r_c$ from the center of mass of the protein is separated from the simulation box. The

analysis of simulations was, therefore, performed by applying the Lorentz condition $\alpha = 0$

$$\chi_c = \chi_c^L \langle \mathbf{M}_0 \cdot \mathbf{M}_t \rangle / \langle \mathbf{M}_0^2 \rangle \tag{69}$$

This limit leads to the appearance of the Lorentz screening factor in front of any correlation involving the dipole moment of the spherical region $\mathbf{M}_t$. From this perspective, cutoff corrections are required to calculate susceptibilities representing the reaction and directing fields discussed above. One obtains for $\chi_R$ and $\chi_D$ in eq 36

$$\begin{aligned} \chi_R &= \frac{\beta}{3} \chi_c^L \langle (\mathbf{E}_s \cdot \hat{\mathbf{m}}_0)(\hat{\mathbf{m}}_0 \cdot \mathbf{M}_t) \rangle \\ \chi_D &= \frac{\beta}{3} \chi_c^L \langle \left(\mathbf{E}_s - \mathbf{E}_\parallel\right) \cdot \mathbf{M}_t \rangle \end{aligned} \tag{70}$$

where $\chi_c^L$ is the static limit of the Lorentz screening (eq 27).

# Results

**Dielectric measurements**. The effect of the protein dipole on both the dielectrophoretic response and the dielectric increment is determined not by the dipole moment itself, but by the scaled parameter $y_0 \propto \langle M_0^2 \rangle / \Omega_0 \propto \langle M_0^2 \rangle / R_0^3$. The result is somewhat sensitive to the definition of the protein volume $\Omega_0 = (4\pi/3) R_0^3$ and the effective radius $R_0$. The algorithm adopted here is to calculate the van der Waals (vdW) volume of the protein and then add the radius of the water molecule 1.43 Å to the vdW radius. The calculated radius is the effective radius of the solvent-accessible surface. Even with this addition, the resulting $y_0$ of the protein is much higher than its bulk analog $y \simeq 6$ for water for all proteins studied here (Table 1). The high value of this parameter is the indication that proteins add polarity to the solution and are expected to produce an increment of the static dielectric constant of solution compared to bulk water. This indeed happens and $\Delta\epsilon/\eta_0$ in eqs 51 is positive for ubiquitin and lysozyme solutions.

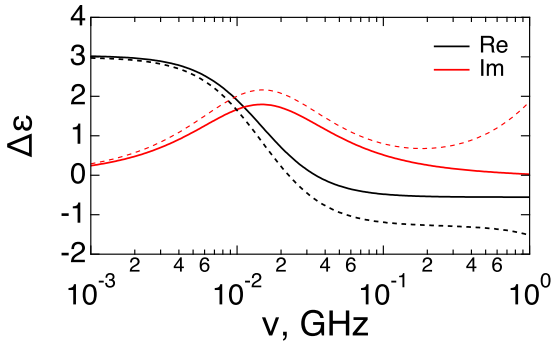


Figure 4: $\Delta\epsilon(\omega)$ reported for $c_0 = 1.14$ mM solution of ubiquitin[30] (dashed lines) and calculated (solid lines) from eq 51 with $y_0 = 154$ from Table 1 and $\tau_r = 10.8$ ns for the protein $\beta$-relaxation (eq 17). The cavity susceptibility $\chi_c = 0.85$ is required to fit the low-frequency part of the difference dielectric spectrum. The black lines mark the real part of $\Delta\epsilon(\omega)$ and the red lines refer to the imaginary part.

Equation 51 is the solution mixture formula yielding the dielectric function of solution at the low protein concentrations allowing to neglect interprotein interactions. This equation is compared in Figure 4 to the reported[30] dielectric increment $\Delta\epsilon(\omega)$ for $c_0 = 1.14$ mM ubiquitin solution. The cavity susceptibility $\chi_c$ was assumed to be constant, the static parameter $y_0$ was taken from Table 1, and the water dielectric function is from independent measurements.[38] Fitting the low-frequency portion of the plot required $\chi_c = 0.85$. There is a discrepancy between the calculated and reported difference dielectric spectra in the region of the water ($\gamma$-relaxation) peak. This might not be related to potential drawbacks of eq 51 since the relaxation time of the $\gamma$-relaxation reported in ref 30 ($\tau_\gamma = 12.5$ ps) deviates from that measured for bulk water[38] ($\tau_\gamma = 8.37$ ps). The water peak does not shift with the addition of the protein at mM concentrations,[39] even though slowing of water's relaxation has been observed in concentrated nonionic solutions.[40]

The value of $\chi_c \simeq 0.85$ can be compared to other sources of this parameter. One can alternatively apply eq 50 connecting $\chi_c$ to the relative dielectric strengths of $\beta$- and $\delta$-relaxation components. Figure 5 shows this calculation for a number of proteins listed in refs 26,30,41. The values of $\chi_c$ are plotted against $M_p^{1/3}$ used to represent the protein size ($M_p$ is the molecular mass). One arrives at $\chi_c \simeq 1.16$. We stress again that according to

eq 46 the appearance of a $\delta$-peak in the dielectric spectrum requires $\chi_c > 1$, in contrast to $\chi_c < 1$ following from the fit presented in Figure 4. This latter calculation is substantially affected by the adopted magnitude of the protein dipole (Table 1) and, to a lesser extent, by the protein volume.

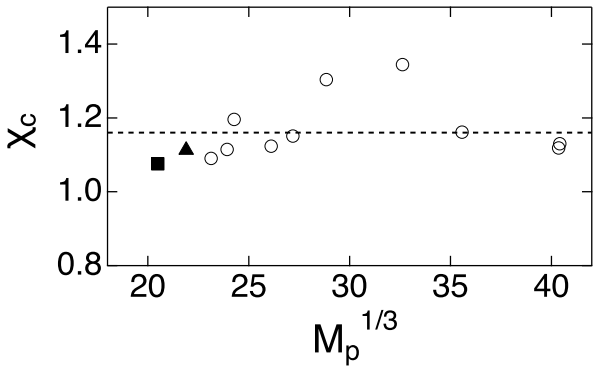


Figure 5: $\chi_c$ calculated from the relative intensities of $\beta$- and $\delta$-relaxation processes according to eq 50 from the data listed in ref[26] (open points). The closed point refers to ubiquitin[30] (square) and RNAse[41] (triangle). The mean value of $\chi_c \simeq 1.16$ is indicated by the horizontal dashed line; $M_p$ is the molecular mass (Da).

The protein volume drops from the calculation if $\Delta\epsilon/\eta_0 \gg \Delta\epsilon_w$ in eq 53. In that case, one can use eq 53, which can be cast in the following form

$$\frac{\Delta\epsilon}{c_0} = 9.13 \times 10^{-5} M_0^2 (2\chi_c - 1) \tag{71}$$

where the numerical factor is calculated for $c_0$ in mM and the protein dipole is in debye units. This equation can be alternatively viewed as the means to determine the protein dipole from the dielectric increment

$$M_0 \simeq 105 \text{ D} \sqrt{\frac{\Delta\epsilon}{c_0(2\chi_c - 1)}} \tag{72}$$

This is the Oncley equation in which the cavity susceptibility replaces an empirical parameter in Oncley's formulation.[42]

Figure 6 shows the dielectric results[9] vs the calculated[43,44] $M_0^2$ for a number of proteins assuming $M_0^2 \simeq \langle M_0^2 \rangle$. This calculation neglects modulations of the protein dipole moment

by conformational fluctuations of the protein. The distributions of the dipole moment magnitudes from MD simulations for the lysozyme (Lys) and ubiquitin (Ubiq) proteins are shown in Figure 7. The width of the dipole moment distribution is about 20% of the most probable value. The error of assuming $M_0^2 \simeq \langle M_0^2 \rangle$ does not exceed 4%.

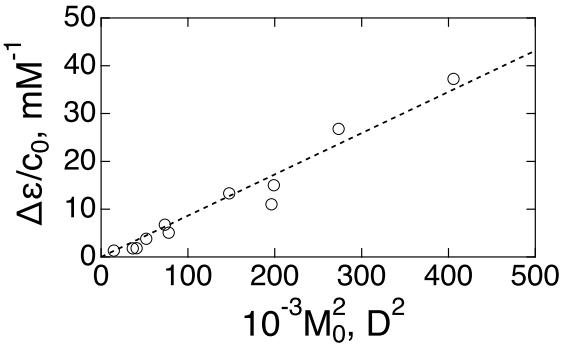


Figure 6: Experimental[9] dielectric increments $\Delta\epsilon/c_0$, $c_0$ is the molar concentration of protein (mM) vs the calculated[43,44] squared dipole moment $M_0^2$. The proteins in the sequence of increasing $M_0$ are: lysozyme, myoglobin, phospholipase, ubiquitin, trypsin, cytochrome $c$, BSA, ribonuclease, RNAse, hemoglobin, carboxypeptidase. The dashed line is a linear fit through the points.

The slope of the plot shown in Figure 6 is consistent with $\chi_c \simeq 0.97$, which falls between $\chi_c \simeq 0.85$ and $\chi_c \simeq 1.2$ from Figures 4 and 6. As mentioned above, both Figures 4 and 6 are affected by the magnitude of the calculated protein dipole. Figure 5 does not depend on this assignment, but is solely based on the assumption that $\delta$-relaxation is associated with cross correlations between the protein and water dipoles.[28,29] Unfortunately, these results cannot be tested against the MD simulations since the correlations $\langle \mathbf{M}_0 \cdot \mathbf{M}_t(r_c) \rangle$ calculated for different radii $r_c$ of the cutoff shells do not convert to a specific limit and still keep rising at the largest shells available from our simulations (Figure S1). Nevertheless, even these results, still affected by the finite size of the simulation cell, give $\chi_c \simeq 0.3 - 0.4$, which are at least an order of magnitude higher than $\chi_c^M \simeq 0.02$ suggested by the dielectric theories (eq 18). All these results indicate that the protein-water Kirkwood factor (eq 21) is close to unity, which is consistent with the values typically found for bulk polar liquids.[14,15] Given the direct connection between $\chi_c$ and the Kirkwood factor, the lack of convergence in direct-space calculations is not surprising since poor convergence of the Kirkwood factor

with increasing the size of the spherical volume around a target dipole is well documented in both analytical theories[12] and simulations.[45] The issue for homogeneous liquids is resolved by taking $k \to 0$ in reciprocal space,[35] which has not been yet accomplished for solute-solvent Kirkwood factors.

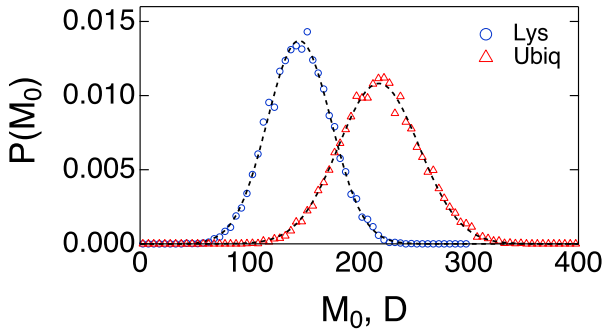


Figure 7: Distribution of the magnitude of the protein dipole. The dashed lines are fits to Gaussian functions with the mean values of 218 D (ubiquitin, Ubiq) and 145 D (lysozyme, Lys) and the Gaussian widths of 37 D (Ubiq) and 29 D (Lys).

As we noted above, $\chi_c$ fully specifies the susceptibility of the protein-water interface $\chi^{\rm int}$ producing the dipole moment $\langle M_z^{\rm int}\rangle_E$ induced in the interface by the external field $E_0$ (eq 28). These values are listed in Table 2 for ubiquitin and lysozyme assuming $E_0 = 0.1$ V/Å. The principal distinction is found between the Maxwell result predicting a negative dipole, lowering the solution polarity, and the positive dipole following from estimates of $\chi_c$ using either MD simulations or the experimental results shown in Figure 5. As mentioned above, the MD calculations for $\chi_c$ are not fully converged due to size restrictions on the water shell in the simulation box and yield underestimated values of $\chi_c$.

**Table 2: Dipole moment $\langle M_z^{\rm int}\rangle_E$ (D) induced at the protein-water interface by the external field $E_0 = 0.1$ V/Å.**

| Protein | M[a] | MD[b] | Exp[c] |
|---|---|---|---|
| Ubiquitin | −3.50 | 0.91 | 1.45 |
| Lysozyme | −5.40 | 0.07 | 1.68 |

[a]Maxwell result from eq 23. [b]From eq 28 with $\chi_c$ from MD. [c]From eq 28 with $\chi_c$ from Figure 5: $\chi_c = 1.08$ (Ubiq) and 1.20 (Lys).

**Local field**. The electric field of the solvent inside the protein is of fundamental signif-

icance for a number of processes. It affects catalytic function,[46–48] rates of protein charge transfer,[49] and line shapes of spectral probes placed inside the protein.[50] The electric field represents collective motions of the entire hydration shell of the protein and thus reports on the shell dynamics. These dynamics are slow as judged from the time correlation function

$$C_E(t) = \langle (\delta \mathbf{E}_s)^2 \rangle^{-1} \langle \delta \mathbf{E}_s(t) \cdot \delta \mathbf{E}_s(0) \rangle \tag{73}$$

where the electric field $\mathbf{E}_s(t)$ is calculated at the center of mass of the protein. The average relaxation times calculated from this correlation function are equal to 6.3 ns for Lys and 4.4 ns for the Ubiq protein (Figure 8 and SI). This result comes in sharp contrast to single-particle dynamics of water molecules in the hydration shell at the picosecond time scale, which are slowed down by a retardation factor relative to bulk water within one order of magnitude.[51–54] Fluctuations of the electric field in bulk water occur on the time scale of longitudinal dielectric relaxation $\simeq 0.2$ ps.[55] The retardation factor of the field inside the protein therefore amounts to 3–4 orders of magnitude.

The local electric field $E_{\rm loc}$ inside the protein carries a different physical meaning. In contrast to the fluctuating solvent field $\mathbf{E}_s$, this is an average field. It represents a cumulative effect of the polarization of the protein dipole and the dipoles of the hydration shell induced by applying an external field to the solution. Since the local field scales linearly with the applied external field $E_0$, the susceptibility $\chi_{\rm loc}$ (eq 37) is the measure of the linear response of the protein and its hydration shell.

The local-field susceptibility in eq 37 is the sum of two components: the reaction-field susceptibility $\chi_R$ and the directing field susceptibility $\chi_D$ (eq 70). Those are listed in Table 3, along with $\chi_c$, for Ubiq and Lys proteins. It is seen that the local field can exceed the external field by about two orders of magnitude. The directing field is also not equal to the cavity field, in contrast to the Onsager assumption used in theories of bulk dielectrics.[19] They do not need to be equal, but are reasonably close in magnitude for dipolar liquids.[20]

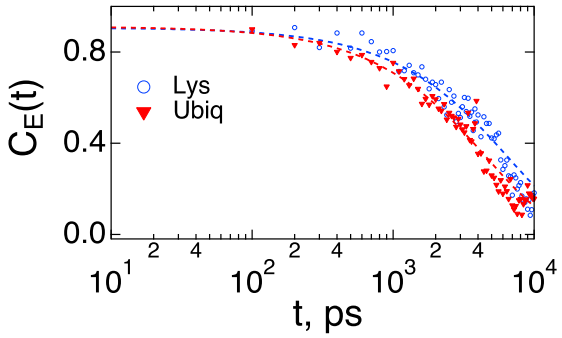


Figure 8: Time correlation functions $C_E(t)$ (eq 73) calculated from 1 $\mu$s MD trajectories for lysozyme (black) and ubiquitin (red). The dashed lines are fits to functions given as sums of exponential and stretched exponential decay functions (see SI). The average relaxation times are: 6.3 ns (Lys) and 4.4 ns (Ubiq).

It is clear that this expectation is not met for proteins in solution. It is important to stress that the cavity field, and not the directing field, has to enter the dielectric constant of the protein solution leading to eq 43 for the dielectric increment. However, when the protein in solution is exposed to electromagnetic radiation, it is the local field at the frequency of radiation that determines its effect on the residues and cofactors inside the protein. Our calculations clearly indicate that the correction of the external field through $\chi_{\rm loc}$ cannot be neglected when low-frequency radiation (with $\omega\tau_r < 1$) is concerned.

We also find that the mean-field approximation for the cavity-field susceptibility $\chi_c$ (eq 39) is in fair agreement with direct calculations (two last columns in Table 3). Both calculations are, however, affected by the need to introduce the spherical cutoff of the hydration shell in the analysis of simulations to replace the dipole moment $\mathbf{M}$ with the dipole moment $\mathbf{M}_t$ of the spherical region surrounding the protein. From this perspective, there is no clear advantage of using one formalism compared to the other. Nevertheless, the numerical agreement between two results offers a route for developing formal theories of $\chi_c$ not relying on the technically challenging calculation of the protein-water Kirkwood factor (eq 21).

**Dielectrophoresis**. Direct measurements of the dielectrophoretic susceptibility have not been accomplished so far, although a number of reports have shown positive dielectrophoresis for proteins at low frequencies (see refs 56,57 for reviews). Equation 60 offers an independent

**Table 3: Local and reaction field susceptibilities for proteins.**

| Protein | $\chi_{\rm loc}$ | $\chi_R$ | $\chi_D$ | $\chi_c{}^a$ | $\chi_c^{{\rm MF}b}$ |
|---|---|---|---|---|---|
| Ubiquitin | 48.4 | 46.5 | 0.92 | 0.36 | 0.38 |
| Lysozyme | 28.9 | 16.4 | 11.5 | 0.37 | 0.39 |

[a]Calculated from MD simulations with the Lorentz cutoff correction according to eq 69.
[b]Calculated from eqs 39 and 70.

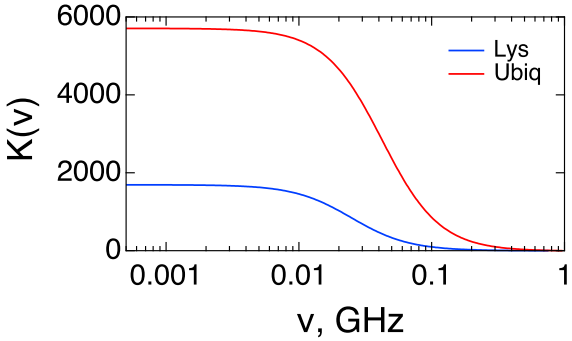


Figure 9: Dielectropheretic susceptibility Re$[K_d(\nu)]$ calculated from eq 29 based on MD simulations, $\nu = \omega/(2\pi)$.

route to this parameter through measurements of the excess static dielectric constant of protein solutions.

Calculations of $K(0)$ from experimental dielectric data according to eq 60 are listed in the third column in Table 1. Dielectric data for ubiquitin were taken for the solution at 1.14 mmol/L,[30] and dielectric data at a similar concentration of 1.9 mmol/L were analyzed for chicken egg-white lysozyme.[31] The results of calculations are sensitive to both the volume of the protein adopted to calculate the volume fraction $\eta_0$ in eq 60 and the value of $\Delta\epsilon(0)$ estimated at zero frequency. In both cases, estimating $\Delta\epsilon(0)$ required extrapolation from the lowest experimental frequency of $\sim 1$ MHz to $\omega = 0$. Hölzel and Pethig[9] have recently reviewed dielectric data for proteins providing values of $\Delta\epsilon(0)/c_0$ for a number of protein solutions, where $c_0$ is the protein molar concentration. These data were used to obtain $K_d(0)$ for cytochrome $c$ listed in Table 1. The lower values of $K_d(0)$ from simulations compared to dielectric experiments are related to underestimated values of $\chi_c$. We find that adopting $\chi_c \simeq 0.8$ brings the results from eq 29 in close agreement with the dielectric estimates from

eq 60.

The frequency dependence of the dielectrophretic susceptibility is calculated by using frequency-dependent dielectric functions and cavity susceptibilities in eq 29 (Figure 9). As mentioned above $\chi_c(\omega)$ is nearly constant and is mostly defined by its static limit. The overall frequency dependence of $K_d(\omega)$ is thus determined by $y_0(\omega)$, which drops from its static limit at the frequency of tumbling of the protein dipole (last column in Table 1).

# Conclusions

Dielectrophoresis of globular proteins in solution, and potentially of other biomolecules, is dominated by the protein dipole moment. The dielectrophoretic susceptibility is many of orders of magnitude higher than the prediction given by the Clausius-Mossotti factor limiting it to the range $-0.5 \leq K \leq 1$. In contrast, the combination of numerical all-atom simulations and the analysis of dielectric results for protein solutions place $K$ of small globular proteins in the range of $10^3 - 10^4$. Dielectrophoresis due to the dipole moment is positive. Negative dielectrophoresis is predicted by dielectric theories (Clausius-Mossotti equation) placing the emphasis on the polarization of the protein hydration shell. These theories assign an overall negative dipole to the hydration shell polarized by the external electric field. Both the atomistic simulations and the analysis of experiment presented here do not support this assignment. The dipole moment of the hydration shell is positive, adding to the dipole moment of the protein polarized by the applied field. The lack of screening by the hydration shell also makes the local field exceed the external field by a substantial factor described by the local field susceptibility. This correction factor needs to be involved when proteins are exposed to low-frequency electromagnetic radiation ($\omega\tau_r < 1$). This result is distinct from our analysis of the cavity field susceptibility (protein-water Kirkwood factor), which is shown to be close to unity and in agreement with the values typically reported for bulk polar liquids. The collective dynamics of the electric field created inside the protein by

hydration water are significantly retarded (4–6 ns) compared to single-particle dynamics of water molecules in the hydration shell.

## Supporting Information Available

Simulation protocol, derivation of finite-size corrections for the analysis of dipolar correlations and cavity-field susceptibility, and the analysis of time correlation functions.

## Notes

The authors declare no competing financial interests.

## Acknowledgement

This research was supported by the National Science Foundation (CHE-1800243, D.V.M.). D.V.M. greatly enjoyed discussing dielectrophoresis with Ronald Pethig.

## References

(1) Pethig, R. *Dielectrophoresis. Theory, Methodology and Biological Applications*; Wiley: Hoboken, NJ, 2017.

(2) Scaife, B. K. P. *Principles of Dielectrics*; Clarendon Press: Oxford, 1998.

(3) Jackson, J. D. *Classical Electrodynamics*; Wiley: New York, 1999.

(4) Matyushov, D. V. Dipolar response of hydrated proteins. *J. Chem. Phys.* **2012**, *136*, 085102.

(5) Fröhlich, H. *Theory of Dielectrics*; Oxford University Press: Oxford, 1958.

(6) Grant, E. H.; Sheppard, R. J.; South, G. P. *Dielectric Behaviour of Biological Molecules in Solution*; Clarendon Press: Oxford, 1978.

(7) Takashima, S. *Electrical Properties of Biopolymers and Membranes*; Adam Hilger: Bristol, 1989.

(8) Nakano, A.; Ros, A. Protein dielectrophoresis: Advances, challenges, and applications. *ELECTROPHORESIS* **2013**, *34*, 1085–1096.

(9) Hölzel, R.; Pethig, R. Protein dielectrophoresis: I. Status of experiments and an empirical theory. *Micromachines* **2020**, *11*, 533–22.

(10) Stratton, J. A. *Electromagnetic Theory*; McGraw-Hill Inc.: New York, 1941.

(11) Landau, L. D.; Lifshitz, E. M. *Electrodynamics of Continuous Media*; Pergamon: Oxford, 1984.

(12) Stell, G.; Patey, G. N.; Høye, J. S. Dielectric constants of fluid models: Statistical mechanical theory and its quantitative implementation. *Adv. Chem. Phys.* **1981**, *48*, 183–328.

(13) Böttcher, C. J. F. *Theory of Electric Polarization, Vol. 1: Dielectrics in Static Fields*; Elsevier: Amsterdam, 1973.

(14) Goldman, S.; Joslin, C. Why hydrogen-bonded liquids tend to have high static dielectric constants. *J. Phys. Chem.* **1993**, *97*, 12349–12355.

(15) Richert, R. Supercooled liquids and glasses by dielectric relaxation spectroscopy. *Adv. Chem. Phys.* **2015**, *156*, 101–195.

(16) Lee, C. Y.; McCammon, J. A.; Rossky, P. J. The structure of liquid water at an extended hydrophobic surface. *J. Chem. Phys.* **1984**, *80*, 4448–4455.

(17) Martin, D. R.; Friesen, A. D.; Matyushov, D. V. Electric field inside a "Rossky cavity" in uniformly polarized water. *J. Chem. Phys.* **2011**, *135*, 084514.

(18) Nee, T. W.; R. Zwanzig, R. Theory of dielectric relaxation in polar liquids. *J. Chem. Phys.* **1970**, *52*, 6353–6363.

(19) Onsager, L. Electric moments of molecules in liquids. *J. Am. Chem. Soc.* **1936**, *58*, 1486–1493.

(20) Martin, D. R.; Matyushov, D. V. Microscopic fields in liquid dielectrics. *J. Chem. Phys.* **2008**, *129*, 174508.

(21) Matyushov, D. V. Response to "comment on 'nonlinear dielectric response of polar liquids' " [J. Chem. Phys. **144**, 087101 (2016)]. *J. Chem. Phys.* **2016**, *144*, 087102.

(22) Matyushov, D. V. In *Nonlinear Dielectric Spectroscopy*; Richert, R., Ed.; Springer: Cham, 2018; pp 1–34.

(23) Böttcher, C. J. F. *Theory of Electric Polarization. Deielctrics in Time-Dependent Fields*; Elsevier, 1973; Vol. 2.

(24) Latypova, L.; Puzenko, A.; Levy, E.; Feldman, Y. Dielectric spectra broadening as a signature for dipole–matrix interactions. V. Water in protein solutions. *J. Chem. Phys.* **2020**, *153*, 045102.

(25) Pethig, R. Protein-water interactions determined by dielectric methods. *Ann. Rev. Phys. Chem.* **1992**, *43*, 177–205.

(26) Miura, N.; Asaka, N.; Shinyashiki, N.; Mashimo, S. Microwave dielectric study on bound water of globule proteins in aqueous solution. *Biopolymers* **1994**, *34*, 357–364.

(27) Wolf, M.; Gulich, R.; Lunkenheimer, P.; Loidl, A. Relaxation dynamics of a protein solution investigated by dielectric spectroscopy. *Biochim. Biophys. Acta (BBA) - Proteins & Proteomics* **2012**, *1824*, 723–730.

(28) Loffler, G.; Schreiber, H.; Steinhauser, O. Callculation of the dielectric properties of a protein and its solvent: Theory and a case study. *J. Mol. Biol.* **1997**, *270*, 520.

(29) Boresch, S.; Höchtl, P.; Steinhauser, O. Studying the dielectric properties of a protein solution by computer simulation. *J. Phys. Chem. B* **2000**, *104*, 8743.

(30) Knocks, A.; Weingärtner, H. The dielectric spectrum of ubiquitin in aqueous solution. *J. Phys. Chem. B* **2001**, *105*, 3635.

(31) Cametti, C.; Marchetti, S.; Gambi, C. M. C.; Onori, G. Dielectric relaxation spectroscopy of lysozyme aqueous solutions: Analysis of the delta-dispersion and the contribution of the hydration water. *J. Phys. Chem. B* **2011**, *115*, 7144–7153.

(32) Seyedi, S. S.; Matyushov, D. V. Protein dielectrophoresis in solution. *J. Phys. Chem. B* **2018**, *122*, 9119–9127.

(33) Hansen, J.-P.; McDonald, I. R. *Theory of Simple Liquids*, 4th ed.; Academic Press: Amsterdam, 2013.

(34) Matyushov, D. V. Dipole solvation in dielectrics. *J. Chem. Phys.* **2004**, *120*, 1375–1382.

(35) Neumann, M. Computer simulation and the dielectric constant at fimite wavelength. *Mol. Phys.* **1986**, *57*, 97.

(36) Abramowitz, M., Stegun, I. A., Eds. *Handbook of Mathematical Functions*; Dover: New York, 1972.

(37) Allen, M. P.; Tildesley, D. J. *Computer Simulation of Liquids*; Clarendon Press: Oxford, 1996.

(38) Vinh, N. Q.; Sherwin, M. S.; Allen, S. J.; George, D. K.; Rahmani, A. J.; Plaxco, K. W. High-precision gigahertz-to-terahertz spectroscopy of aqueous salt solutions as a probe of the femtosecond-to-picosecond dynamics of liquid water. *J. Chem. Phys.* **2015**, *142*, 164502–8.

(39) Yanase, K.; Arai, R.; Sato, T. Intermolecular interactions and molecular dynamics in bovine serum albumin solutions studied by small angle X-ray scattering and dielectric relaxation spectroscopy. *J. Molec. Liq.* **2014**, *200*, 59–66.

(40) Levy, E.; Puzenko, A.; Kaatze, U.; Ben Ishai, P.; Feldman, Y. Dielectric spectra broadening as the signature of dipole-matrix interaction. I. Water in nonionic solutions. *J. Chem. Phys.* **2012**, *136*, 114502.

(41) Oleinikova, A.; Sasisanker, P.; Weingärtner, H. What can really be learned from dielectric spectroscopy of protein solutions? A case study of Ribonuclease A. *J. Phys. Chem. B* **2004**, *108*, 8467.

(42) Oncley, J. L. The investigation of proteins by dielectric measurements. *Chem. Rev.* **1942**, *30*, 433–450.

(43) Takashima, S. Electric dipole moment of globular proteins: measurement and calculation with NMR and X-ray databases. *J. Noncrystal. Solids* **2002**, *305*, 303–310.

(44) Takashima, S.; Asami, K. Calculation and measurement of the dipole moment of small proteins: Use of protein data base. *Biopolymers* **1993**, *33*, 59–68.

(45) Linse, P.; Karlström, G. Dipolar order in molecular fluids: II. Molecular influence. *J. Stat. Phys.* **2011**, *145*, 418–440.

(46) Warshel, A.; Sharma, P. K.; Kato, M.; Xiang, Y.; Liu, H.; Olsson, M. H. M. Electrostatic basis for enzyme catalysis. *Chem. Rev.* **2006**, *106*, 3210–3235.

(47) Fried, S. D.; Bagchi, S.; Boxer, S. G. Extreme electric fields power catalysis in the active site of ketosteroid isomerase. *Science* **2014**, *346*, 1510–1514.

(48) Fried, S. D.; Boxer, S. G. Response to comments on "extreme electric fields power catalysis in the active site of ketosteroid isomerase". *Science* **2015**, *349*, 936–936.

(49) Martin, D. R.; Dinpajooh, M.; Matyushov, D. V. Polarizability of the active site in enzymatic catalysis: Cytochrome c. *J. Phys. Chem. B* **2019**, *123*, 10691–1069.

(50) Fried, S. D.; Boxer, S. G. Electric fields and enzyme catalysis. *Ann. Rev. Biochem.* **2017**, *86*, 387–415.

(51) Laage, D.; Elsaesser, T.; Hynes, J. T. Water dynamics in the hydration shells of biomolecules. *Chem. Rev.* **2017**, *117*, 10694–10725.

(52) Qin, Y.; Zhang, L.; Wang, L.; Zhong, D. Observation of the global dynamic collectivity of a hydration shell around apomyoglobin. *J. Phys. Chem. Lett.* **2017**, *8*, 1124–1131.

(53) King, J. T.; Arthur, E. J.; Osborne, D. G.; Brooks III, C. L.; Kubarych, K. J. Biomolecular hydration dynamics probed with 2D-IR spectroscopy: From dilute solution to a macromolecular crowd. *Chinese Chem. Lett.* **2015**, *26*, 435–438.

(54) Perticaroli, S.; Ehlers, G.; Stanley, C. B.; Mamontov, E.; O'Neill, H.; Zhang, Q.; Cheng, X.; Myles, D. A. A.; Katsaras, J.; Nickels, J. D. Description of hydration water in protein (green fluorescent protein) solution. *J. Am. Chem. Soc.* **2017**, *139*, 1098–1105.

(55) Samanta, T.; Matyushov, D. V. Mobility of large ions in water. *J. Chem. Phys.* **2020**, *153*, 044503.

(56) Pethig, R. Limitations of the Clausius-Mossotti function used in dielectrophoresis and electrical impedance studies of biomacromolecules. *ELECTROPHORESIS* **2019**, *5*, 024116–9.

(57) Hayes, M. A. Dielectrophoresis of proteins: experimental data and evolving theory. *Anal. Bioanal. Chem.* **2020**, *115*, 7144.

# TOC Graphic